ELSEVIER

Stress-assisted discontinuous grain growth and its effect on the deformation behavior of nanocrystalline aluminum thin films

D.S. Gianola [a], S. Van Petegem [b], M. Legros [c], S. Brandstetter [b],
H. Van Swygenhoven [b], K.J. Hemker [a],*

[a] *Mechanical Engineering, Johns Hopkins University, 101 Latrobe , 3400 N Charles Str., Baltimore, MD 21218 2686, USA*
[b] *Paul Scherrer Institute, CH-5232, Villigen-PSI, Switzerland*
[c] *CEMES-CNRS, 31055 Toulouse, France*

Abstract

Unique mechanical properties have been measured in submicrometer freestanding nanocrystalline Al films, where discontinuous grain growth results in a fundamental change in the way in which the material deforms. In contrast to the limited ductility normally associated with nanocrystalline metals, these nanocrystalline films exhibit extended tensile ductility. In situ X-ray diffraction and postmortem transmission electron microscopy point to the importance of stress-assisted room temperature grain growth in transforming the underlying processes that govern the mechanical response of the films: nanoscale deformation mechanisms give way to microscale plasticity.
© 2006 Acta Materialia Inc. Published by Elsevier Ltd. All rights reserved.

Keywords: Nanocrystalline materials; Mechanical properties; Grain boundary migration; Plastic deformation; Thin films

1. Introduction

Guaranteeing the reliability of next-generation micro- and nanoscale devices will require fundamental descriptions of their mechanical behavior. To be truly predictive these descriptions must be based on a detailed understanding of the deformation mechanisms that operate at reduced length scales. The fact that these mechanisms have not been clearly identified for metallic materials with grain sizes of less than 100 nm is currently exacerbated by the realization that many of the plasticity models developed to describe microcrystalline metals and alloys are known to break down at these grain sizes [1–3]. Moreover, recently observed room temperature grain growth may greatly influence the mechanical response of nanocrystalline structures, but the reason for this growth and its effect on mechanical behavior have not been elucidated.

Plastic deformation in metals and alloys is most often governed by dislocation generation and multiplication, which are highly susceptible to size effects. Unusual deformation behavior and mechanical properties have been reported in studies where intrinsic microstructural features are confined to the nanometer scale and where the physical dimensions of samples are reduced to the microscale (see for example Refs. [4–12]). The intrinsic effects generally result in a concomitant increase in strength and loss of ductility, especially in polycrystalline metals with nanometer-sized grains. A few exceptions where high strength and good ductility coexist have been reported [13,14], but the general lack of ductility of nanocrystalline metals is understood to be related to the increased difficulty associated with operating dislocation sources within extremely small grains.

Molecular dynamics (MD) simulations suggest that nanocrystalline metals accommodate external loads by means of grain boundary sliding and the emission of dislocations that traverse the grain and are absorbed into the

---

* Corresponding author. Tel.: +1 410 516 4489.
E-mail address: hemker@jhu.edu (K.J. Hemker).

opposite grain boundary without multiplying or interacting with other dislocations [15–18]. This view is consistent with postmortem transmission electron microscopy (TEM) observations [5,6,19] and in situ X-ray diffraction experiments [20], which indicate that permanent dislocation networks are not built up during plastic deformation. The emerging picture is that the ductility of nanocrystalline metals is limited by the lack of dislocation multiplication mechanisms and the required operation of less efficient deformation processes, such as grain boundary sliding and dislocation emission from grain boundaries.

Mechanistic descriptions that have been developed to describe nanocrystalline metals have generally considered the microstructure to be stable, but there is emerging evidence to suggest that this is not always the case. In situ nanoindentation of ultrafine-grained and nanocrystalline Al films deposited on specially designed Si wedges demonstrated rapid grain boundary migration and coalescence during deformation [21]. Another study has reported the grain growth of ultrafine-grained and nanocrystalline Cu near the indented region during microhardness testing at both cryogenic and room temperatures, and diminishing values of hardness with increasing indenter dwell time have been attributed to this microstructural evolution [22].

Here we report on the observation of high strength and unusually high room temperature ductility in submicrometer freestanding nanocrystalline Al thin films. In situ X-ray diffraction and TEM analyses demonstrate stress-induced grain growth as a room temperature mechanism that facilitates tensile deformation and directly influences the macroscopic mechanical behavior. We argue that the unusual response of the films is directly related to this growth process, which results in the continuous production of defect-free grains. Unable to explain this growth with traditional driving forces, we have come to attribute stress coupled grain boundary motion as the catalyst for the grain growth.

2. Experimental

2.1. Thin-film synthesis and sample fabrication

Physical vapor deposition methods are viable means of synthesizing high-quality nanocrystalline films using one-step processing. High-purity nanocrystalline Al thin films were synthesized using pulsed DC-magnetron sputtering. Films with thicknesses of 180–380 nm and average grain sizes of 40–90 nm were fabricated. Film deposition using an Al target (99.999% purity) was interrupted in intervals of $\sim$20 nm to minimize the growth of columnar grains. For the majority of samples, a base pressure of 10^{-7} torr was achieved in the chamber, and an argon pressure of 6 mtorr was used at a flow rate of 42.7 cm^3/s during sputtering, although films deposited at higher base pressures (10^{-6} torr) were studied to determine the influence of impurities. A gun current of 100 mA was used with a motorized sample stage to allow for even exposure to the incident flux resulting in good thickness uniformity. Pulsed deposition

was performed with an on-time and an off-time of 1 min each for all deposition runs.

Surface and bulk micromachining techniques were used to fabricate micro-tensile test structures that alleviate the challenges usually associated with the direct mechanical testing of submicrometer freestanding thin films. These methods allow for the creation of high-purity, high-quality films, well-defined sample geometry, and batch processing. The gage section of the resultant film spans across a "frame" of (0 0 1) Si with an etched backside window and support strips on the periphery (Fig. 1). The frame allows for safe handling of these fragile films, and the support strips were cut using a diamond blade just prior to elongation.

The process flow for fabricating the samples began with a 4 μm thick thermal SiO$_2$ layer that was grown on a Si wafer and used as a mask for backside window etching. Using KOH as an anisotropic etchant, a window was defined on the backside of the specimen that allows for the release of the gage section. The backside etch was stopped with $\sim$50 μm of Si remaining to provide support for frontisde patterning and film deposition. Then, a liftoff technique was employed to pattern the microsample geometry on the frontside using positive photoresist. The desired nanocrystalline metallic film was then sputtered on top of the photoresist and the resulting geometry was defined by the photoresist, which was dissolved away in acetone. Since dicing of a brittle Si wafer into individual test dies is cumbersome, lines were patterned around the outside of the specimen with a thickness such that the KOH etchant closed a v-groove channel at a calculated depth; greatly simplifying separation of the dies along preferred Si crystallographic orientations. Finally, a pulsed dry gas etchant of XeF$_2$, which imparts a high selectivity of Si to Al [23], was used to remove the supporting Si layer (at a rate of approximately 2 μm/min) to reveal the freestanding thin film.

2.2. Material characterization

Several techniques were employed to characterize precisely the thin films and their corresponding microstructure in both their as-deposited and deformed configurations.
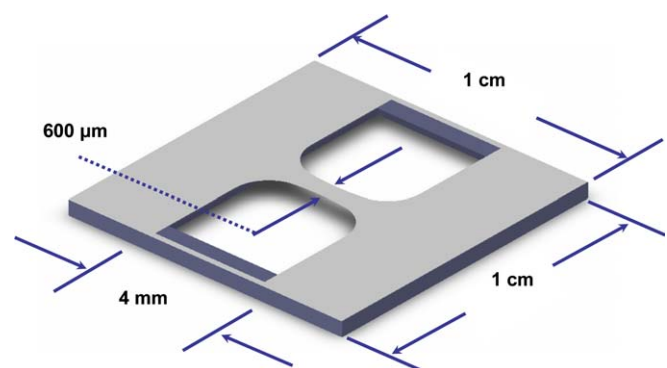

Fig. 1. Schematic of the framed thin-film microsample used for mechanical testing.

Microstructural morphology was characterized primarily using TEM in both bright- and dark-field modes, although scanning electron microscopy was utilized to ensure the continuity and coherency of grains. No additional steps were required to achieve electron transparency in the thin-film samples, eliminating the possibility of preparation artifacts. A statistical treatment of the grain sizes in the films, involving the compilation of grain size distributions, comparisons to analytical functions (e.g. lognormal), and the analysis of the ratio of the mean to standard deviation ratios, was applied to evaluate the composite-like nature, and a number of measurements of in-plane grain sizes from bright-field TEM images were consequently used. All grain size distributions presented herein represent a minimum of 400 measurements of size.

Cross-section TEM samples were prepared from the as-deposited material to determine the through-thickness grain morphology. Samples representing all studied thicknesses showed no dominance of columnar grain structures; several grains through the thickness of the films were observed. In addition, TEM tilting experiments revealed an abundance of overlapping grains, indicating that columnar grains were not prevalent. X-ray pole figure analysis using a four-circle diffractometer did not give evidence of any strong texture, but the presence of weaker textures could not be ruled out since the thin films yielded low diffracted intensity for the Cu Kα radiation used in this setup, resulting in low signal-to-noise ratios. Film thickness was measured using a Dektak IIA stylus profilometer for each specimen, and was found to agree well with measurements of the cross-section TEM samples.

2.3. Microsample tensile testing and in situ peak profile techniques

The tensile experiments conducted for this study were performed using two independent test frames. A dedicated thin-film microsample tensile testing apparatus was constructed at Johns Hopkins University and used for the majority of experiments; details for this setup are given in Ref. [24]. A similarly constructed device was used for all in situ X-ray measurements at the Swiss Light Source and is described in Ref. [20]. All in situ and ex situ tension tests were conducted at rates of $\dot{\varepsilon} = 2 \times 10^5$ and $5 \times 10^{-5}\,\mathrm{s}^{-1}$, respectively, and all deformed specimens were retained for postmortem TEM observations. The repeatability of the stress–strain curves measured in this study was confirmed by comparing the results of multiple samples obtained using both machines, as demonstrated in Fig. 2. Strain was obtained directly by measuring the displacement of the sample grips using a capacitance gage (0.1 μm resolution) and an optical extensometer (subpixel resolution) for the ex situ and in situ tension tests, respectively. In addition, a digital image correlation (DIC) system was implemented to track the evolution of deformation during tensile testing. The results of these experiments demonstrate that grip displacement is an adequate measure
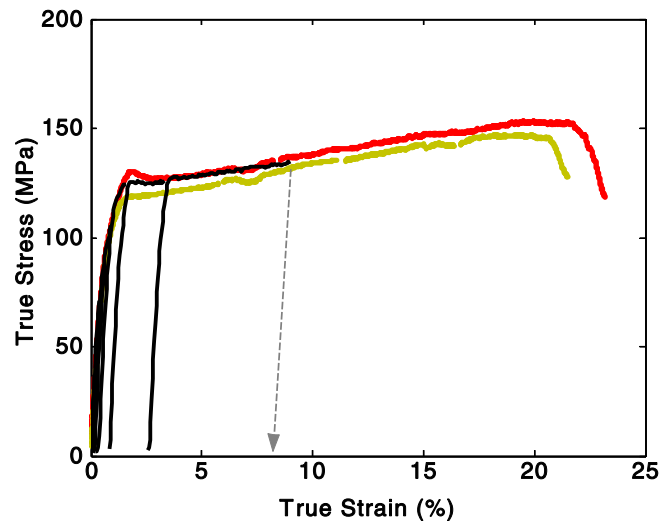

Fig. 2. Set of representative stress–strain curves for the 380 nm films demonstrating the repeatability of the obtained results. The black curves were measured during load–unload experiments using the in situ X-ray technique at the Swiss Light Source, and the tensile straining of this sample was terminated prior to failure for microstructural investigation. All other curves, showing tensile elongations to failure in excess of 20%, were measured using the microsample tensile testing setup at Johns Hopkins University.

for the nominal strain in the sample during the majority of deformation, although during periods of tensile instability (global and local necking), sample strains were measured to be as much as twice that measured using grip displacement. For the sake of clarity, all strains reported herein represent nominal strain in the sample as measured from grip displacements and typically underestimate the total strain to failure.

The high intensity of the Swiss synchrotron light source and the development of a microstrip detector covering a diffraction angle of 60° with an angular resolution of 0.0037° allowed for the measurement of the entire X-ray diffraction pattern at once during continuous deformation without having to scan sequentially the angular range of the scattering angle. Peak profile analyses of numerous Bragg diffraction peaks were followed in situ during deformation and changes in the width of these peaks were used to characterize the underlying deformation mechanisms. In the current study, a monochromatic X-ray beam of 17.5 keV was focused on the central part of the gage, illuminating an area of about 0.5 mm in diameter.

3. Results

3.1. Effect of stress-assisted grain growth on mechanical behavior

The tensile tests conducted in this study uncovered two distinct types of mechanical behavior and representative curves for each are shown in Fig. 3 The first type of behavior is illustrated by the curve exhibiting the highest flow strength and lowest strain to failure (curve 1). The strength

of this film, which is 15–20 times higher than the strength of coarse-grained aluminum [25], the gradual deviation from elastic behavior that occurs in the early stages of plastic deformation, the limited elongation, and the dramatic strain softening that occurs upon tensile flow localization are all attributes that have previously been associated with nanocrystalline metals [12,26–29].

By contrast, the majority of specimens tested in this study exhibited intermediate strengths, more pronounced deviation from linear elasticity, and the unexpected development of a region of extended plasticity (curve 2). The strain hardening rate in this region was found to be remarkably low and constant and the flow strength and strain to elongation of these specimens were observed to vary with film thickness and the as-deposited grain size as shown in Table 1; thinner films exhibited higher strength and less ductility. This size effect is illustrated by comparing the 380/90 behavior (curve 3), in which strains to failure easily reached 20% elongation, with the 180/40 results (curve 2) shown in Fig. 3.

The most dramatic difference in the two types of behavior was that some specimens developed a region of extended plasticity and some did not. Postmortem TEM observations (Figs. 3(b) and (c)) provided an insight into the microstructural changes that govern these two types of mechanical behavior. A qualitative comparison of the microstructures of specimens that showed high strength and limited ductility with those that showed intermediate strength and extended plasticity shows an obvious disparity: discontinuous grain growth occurred in specimens that exhibit behavior with regions of extended plasticity, while no drastic microstructural evolution was observed in samples that retain nanocrystalline type behavior.

TEM micrographs of the as-deposited and plastically deformed 380 nm films (Fig. 4) provide a more detailed view of the processes associated with the extended plasticity that was realized in a majority of the tensile experiments. Direct comparison of the as-deposited microstructure (Fig. 4(a)) with those observed after 9% and 23% deformation (Figs. 4(b) and (c)) provides clear evidence of discontinuous grain growth, the number of large grains scaling with the plastic strain. These bright-field observations are reinforced by the selected-area diffraction patterns (using similar selected areas for each pattern) that show a
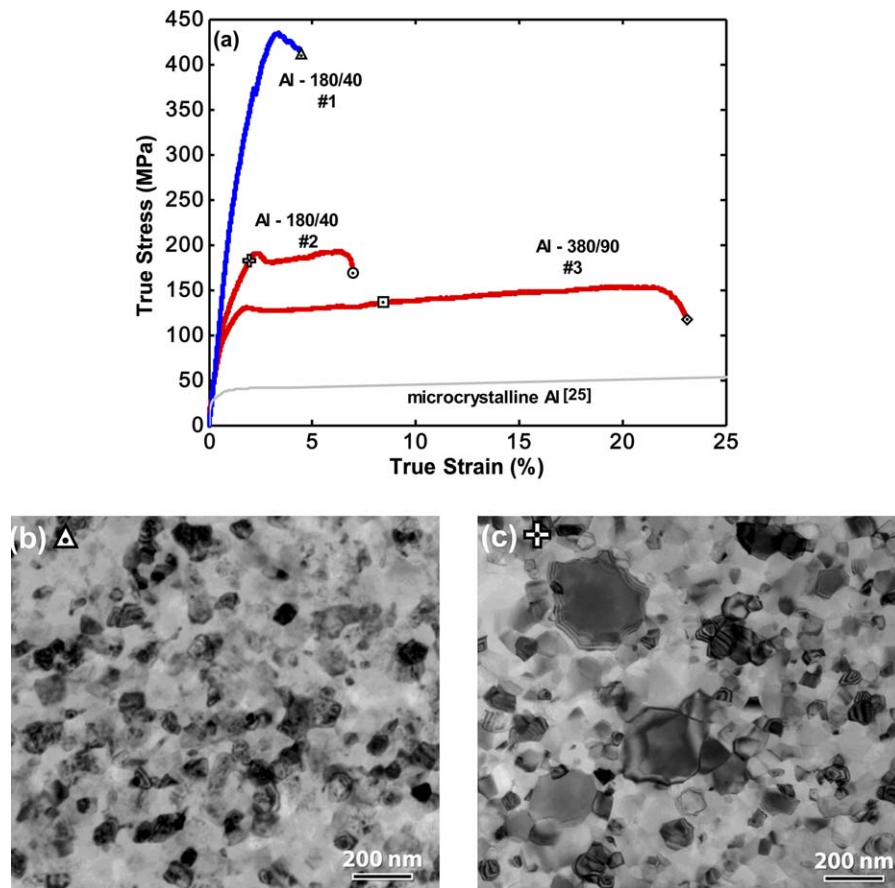

Fig. 3. (a) Representative stress–strain curves illustrating two different types of tensile behavior of submicrometer freestanding nanocrystalline aluminum films with a thickness and mean grain size of 180 and 40 nm and a third with a thickness and mean grain size of 380 and 90 nm. The open symbols correspond to the points where postmortem TEM observations were conducted. (b,c) Bright-field TEM images showing microstructures for two deformed 180 nm samples. The microstructure in (b) corresponds to curve 1 and minimal grain growth was detected. By contrast, the microstructure in (c), which corresponds to curve 2, exhibited obvious grain growth, even at 2% strain.

Table 1
Results of room temperature Al thin-film tensile testing

Sample batch	Film thickness (nm)	Initial grain size (nm)	Yield stress at 0.2% offset (MPa)	Ultimate tensile strength (MPa)	Elongation at fracture (%)
Grain growth					
180/40	187 ± 7	38 ± 16	116 ± 14	190 ± 8	7.0
380/90	367 ± 17	95 ± 33	91 ± 9	149 ± 7	22.4 ± 1.2
No grain growth					
180/40	187 ± 7	38 ± 16	287	434	5.2
165/60	165 ± 2	62 ± 26	271	398	5.5

transition from continuous diffraction rings in the as-deposited sample to more discrete spots in the deformed films. Direct in-plane measurements from the TEM images for the deformed samples demonstrate that 400–500 nm grains were embedded in a sea of smaller grains with the original grain size distribution. The difference in microstructure between 9% and 23% strain lies predominantly in an increased number of larger grains (those with a mean size of approximately 400 nm) and not in an increase in grain size of these existing larger grains. In other words, the grain size distribution became mixed-modal during loading, and upon further loading the matrix of smaller grains grew in a similar discontinuous way while the larger mode remained relatively constant. This observation is consistent with thin-film constraints that place an upper bound on the grain size [30–33].

The as-deposited microstructure was dislocation-free, but the formation of dislocation networks was observed in the larger grains of the deformed samples (Fig. 4(d)). Observations of well-defined individual dislocations were rare but tangled groups of dislocations were common. These dislocation networks were observed in a substantial percentage of the large grains, and the dislocation density was found to be qualitatively higher in the sample that was strained to 23% than in the one strained to only 9%.

3.2. Role of the applied stress on grain growth

A quantitative measure of the grain growth that occurred during deformation is illustrated in the form of grain size distributions in Fig. 5. Direct comparisons of the distributions of the as-deposited and deformed samples demonstrate the discontinuous grain growth that has occurred in samples that exhibit extended plasticity. In addition, TEM measurements obtained outside of the gage section of the specimen (in a region with much lower stress
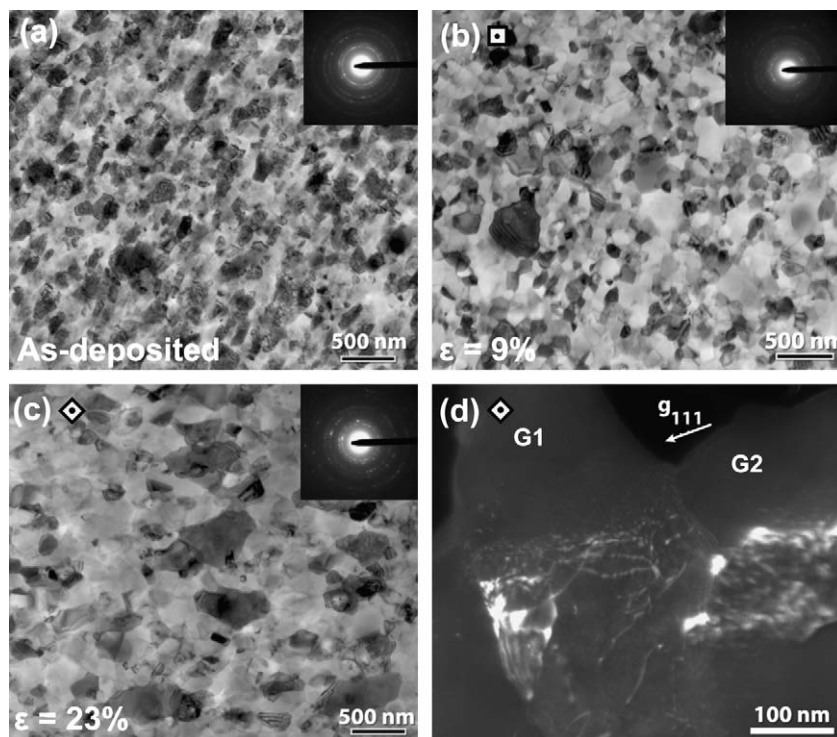

Fig. 4. Bright-field TEM images showing the evolution of stress-assisted grain growth in 380 nm films for (a) undeformed, (b) 9% strained, and (c) 23% strained microstructures. (d) A weak-beam dark-field TEM image of a sample deformed to 23% strain illustrating dislocation tangling and storage. Dislocation debris was observed in a majority of the large grains, and the dislocation density in grain G1 was estimated to be $\sim10^{13}$ cm^{-2}.
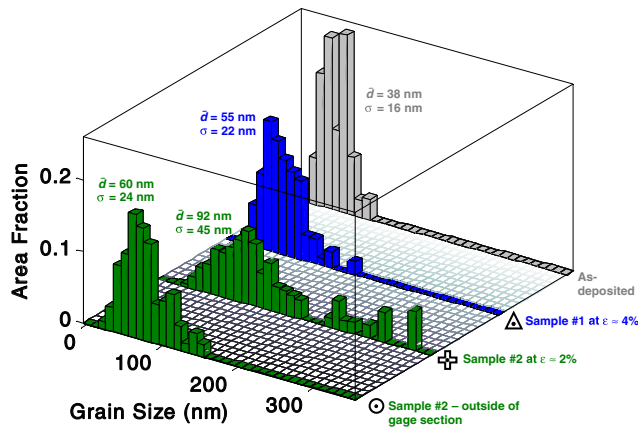
Fig. 5. Area fraction histograms of grain size as measured from TEM images showing evolution of stress-assisted coarsening as compared with the as-deposited microstructure. Distributions obtained within and outside of the gage section for sample 2 indicate the importance of stress in triggering grain growth.

during testing) showed a grain size distribution resembling that of the as-deposited material. The association of widespread grain growth with tensile loading and the observation that this growth is limited to the gage section of these specimens points to the importance of the applied stress in promoting the grain growth observed in this study. In the current study the influence of the applied stress has also been evidenced through in situ TEM straining experiments of 380 nm thick nanocrystalline Al films; grain growth is observed at the tip of slow-growing cracks but not in the other regions of the thin foil. Taken as a whole these experimental observations all point to the importance of the applied stress in triggering grain growth in these nanocrystalline structures. The role of the stress can also be inferred from previously reported observations of localized room temperature grain growth during indentation studies of nanocrystalline Cu [22] and nanocrystalline Al [21], although the results from these previous studies were not as unambiguous because the large stress gradient under the indenter provides an additional driving force for this growth.

3.3. In situ peak profile experiments

In order to further elucidate the deformation mechanisms, the nanocrystalline thin films were deformed in situ at the Swiss Light Source and the position and broadening of multiple Bragg diffraction peaks were recorded during deformation. X-ray peak profiles for the (111), (200), (220), and (311) diffraction peaks of the 380 nm thick film were analyzed using similar software as reported in [20]. The evolution of the full width at half maximum (FWHM) values of the (111) Bragg peak is contrasted with the stress–strain behavior in Fig. 6. The first few load–unload cycles were conducted in the linear-elastic regime, and variations in the peak broadening of the different peaks were measured. The observed differences in inho-

mogeneous strain accommodation (the FWHM of the (111) peak and the (200) peaks do not increase, whereas broadening starts to be observed for the (220) and the (311) reflections) are consistent with theoretical models based on elasticity, which predict that under certain conditions (e.g. no texture and strain is described by a weighted average of the strain calculated under the assumptions of strain (Voigt) and stress (Reuss) continuity) peak broadening due to elastic anisotropy only shows up in certain families of peaks [34].
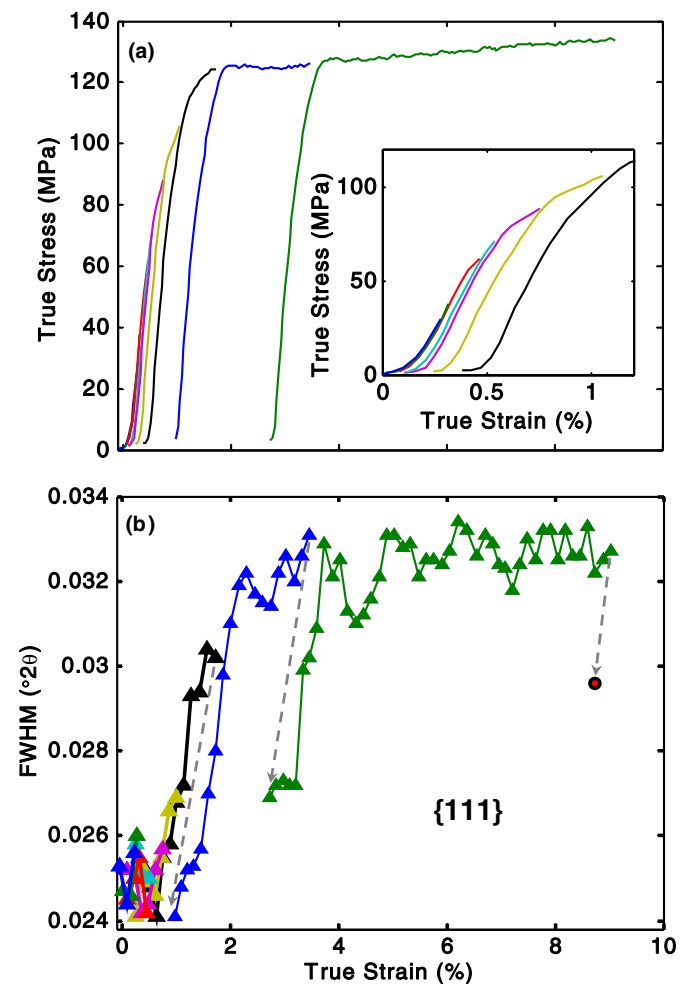

Fig. 6. Stress–strain behavior correlated with in situ X-ray peak broadening in a series of load–unload tensile tests on a 380 nm film. The inset in (a) shows the first several loading cycles and demonstrates the progression from elastic to plastic behavior. The Bragg diffraction peaks were tracked continuously over an angular range of 60° (2θ) during these experiments and the FWHM was measured as a function of applied strain. (b) Broadening data are shown for the {111} peak. The reversible nature of the FWHM in the early cycles (up to and including the black curve) is indicative of nanoscale deformation mechanisms, while the development of irreversible peak broadening (blue and green curves) suggests a transition to microcrystalline plasticity. The specimen did not fail but was unloaded at 9% strain and used for TEM characterization. This behavior is consistent with all measured crystallographic peaks. (For interpretation of the references to colour in this figure legend, the reader is referred to the web version of this article.)

Cyclic loadings that extended just beyond the elastic limit (magenta, olive, and black curves) resulted in steadily increasing but fully reversible peak broadening. This observation of plastic deformation without permanent peak broadening is similar to that reported for electrodeposited nanocrystalline Ni [20] and is indicative of nanocrystalline deformation mechanisms that avoid dislocation interactions and intragranular dislocation storage.

The peak broadening increased substantially during the early stages of extended plasticity (blue curve) and then remained approximately constant (green curve). Unloading at 3% and 9% strain revealed the development of a non-reversible component of peak broadening that suggests a transition from nanocrystalline to more traditional micro-crystalline deformation mechanisms involving dislocation tangling and storage, as evidenced by the TEM observations of the sample strained to 9%. The saturation in peak broadening in the region of extended plasticity may be explained by the competition between two mechanisms: grain growth that reduces the FWHM and dislocation activity that increases the FWHM.

In addition to tracking the evolution of the peak broadening during deformation, the peak position can give indirect information about the deformation processes that are occurring. The peak position, which provides an estimate of the mean elastic strain in the sample as regards the interplanar spacings is shown as a function of strain in Fig. 7 for both (1 1 1) and (2 2 0) peaks. The peak position increased monotonically during each loading cycle, showing an initial linear behavior representing elastic deformation, and deviated from linearity in accordance with the stress–strain behavior. The peak shift saturated at the approximate onset of the extended plastic region, and only slight increases were measured during this regime. These increases beyond the elastic response are most likely indications of the composite-like nature of deformation when discontinuous growth has occurred, in which large grains are deforming plastically (no corresponding peak shift), while small grains are accommodating deformation by elastic processes.

4. Discussion

4.1. Influence of discontinuous grain growth on mechanical behavior

TEM observations of the 180 nm samples (see for example Fig. 3) indicate that grain growth does not occur in all samples (approximately 80% of samples measured in this study showed grain growth after deformation), but when it does, growth commences in the early stages of plastic deformation and is crucial for the formation of the region of extended plasticity. Measurements of high initial strain hardening, a high ultimate strength, flow softening, and limited plasticity are associated with the presence of a stable nanocrystalline microstructure. By contrast, samples that undergo discontinuous grain growth exhibit very dif-
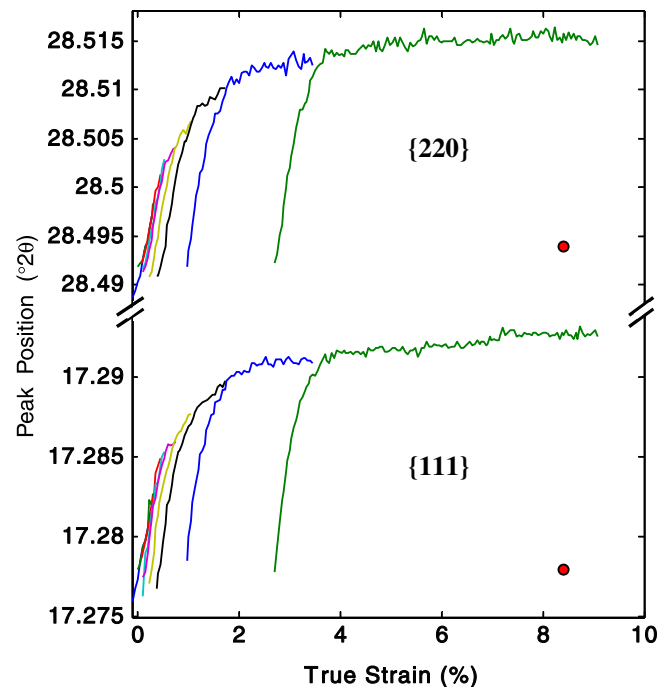

Fig. 7. Peak position as a function of true strain in the series of load–unload tests illustrated in Fig. 6 for the {1 1 1} and {2 2 0} peaks. The peak position monotonically increases for each loading cycle, and the deviation from linearity shows the transition from elastic to plastic processes.

ferent mechanical behavior. The larger grains are initially dislocation-free (Fig. 3(c)) but facilitate dislocation-based microcrystalline plasticity, as evidenced by the observation of dislocation debris formation and irreversible peak broadening at larger strains. Similar behavior was exhibited in the 380 nm films, and the flow stress in these samples appeared to scale with the grain size, which is governed by the film thickness. A comprehensive description of the stress–strain behavior will require the development a composite-like model of hard (original small-grained) and soft (large-grained) regions, but the onset of extended plasticity appears to be related to an achieved percolation or connectivity of large grains. Such a model describing yield behavior of nanocrystalline materials was recently developed within a micromechanics framework to account for a distribution of grain sizes [35]. The utility of this model is clearly demonstrated in systems with a static microstructure during the course of deformation, but the lognormal distribution that was used does not physically capture the discontinuous microstructural evolution observed in this study.

Rapid grain coarsening in nanocrystalline Cu under a microhardness indenter was observed in a recent investigation at both ambient and cryogenic temperatures [36]. In that study it is interesting to note that grain coarsening and the associated hardness relaxation occurred more rapidly at cryogenic temperatures than it did at room temperature. This phenomenon can be attributed to the elevated stresses that are required to induce plastic processes [37] at these temperatures. These experiments confirm that the

mechanisms for growth are primarily stress driven, not diffusion or thermally driven.

4.2. Driving forces for grain growth

In general, the driving force for grain growth is related to a material's desire to reduce its overall free energy. This reduction is traditionally manifest as a decrease in grain boundary energy, stored deformation energy, surface energy, or elastic strain energy [38]. The importance of applied stress and the observation of discontinuous, not continuous, grain growth suggest that additional factors play an important role in initiating and promoting the grain growth that has been observed. It is, however, instructive to consider the traditional driving forces for grain growth before considering additional causes.

If reductions of grain boundary energy alone drive growth, then the kinetics of growth in two dimensions would proceed in a manner dictated by the relation $d\bar{r}/dt \propto \overline{M}\bar{\gamma}_{gb}/\bar{r}$, where $\bar{r}$ is the average in-plane grain radius, $\overline{M}$ is the average grain boundary mobility with a temperature dependence that can be expressed in an Arrhenius form, and $\bar{\gamma}_{gb}$ is the average grain boundary energy [38]. This relation suggests that the grain radii will increase homogeneously with $t^{1/2}$ and that the shape of the grain size distribution is time-invariant, which is not observed in the stress-assisted discontinuous growth reported in this work. The ratio of the mean grain size to the standard deviation of the distribution changes as a function of the applied deformation, indicating that subpopulations of grains are growing at the expense of others.

Given the thin-film geometry employed in the current study, crystallographic variations in surface energy might be expected to promote the growth of favorably oriented grains. The minimization of surface energies during the growth of grains could lead to a texture in polycrystalline films. The (111) orientation in fcc Al is thought to minimize this surface energy [30]. However, orientation mapping in TEM of the resultant large grains suggests that grains with low energy, e.g. (111) oriented grains, are not preferred (Fig. 8). Instead, the grain orientations seem to be randomly distributed and do not favor a (111) texture.

Grain-to-grain differences in strain energy would also promote discontinuous grain growth [30], but the relatively isotropic elastic behavior of Al (which can be defined by the anisotropy ratio of the elastic constants, or $A = (C_{11} - C_{12})/2 - C_{44}$, where $A = 1$ for a perfectly isotropic material and $A = 1.2$ for Al) is expected to mitigate this effect in the current study. Preliminary calculations of the driving force that may arise associated with variations in elastic strain energy indicate that it is as much as four orders of magnitude lower than those driving forces corresponding to surface energy and grain boundary line tension.

TEM observations show no evidence of stored dislocation networks in both the as-deposited microstructures and evolved microstructures with extensive growth prior
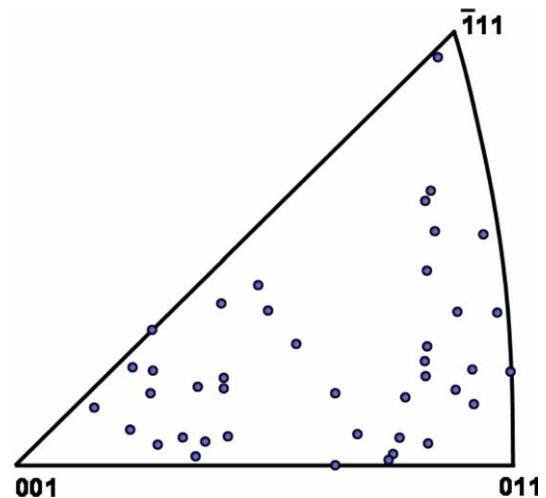

Fig. 8. Inverse pole figure showing orientations of coarsened grains after deformation of a 380 nm film, determined using TEM. The orientations are randomly distributed throughout the triangle.

to the onset of the extended plasticity regime. Only once the grains have grown to a size at which normal dislocation tangling can occur do these networks remain for postmortem observation, which suggests that the effect of stored deformation as a driving force for incipient growth is negligible. Even the dislocation densities calculated from TEM images of fractured samples in which grain growth has already occurred do not provide a substantial enough driving force to be a significant effect. These observations confirm the fact that the applied stress plays an important role in promoting grain growth.

4.3. Role of stress-coupled grain boundary migration

Our inability to explain the observed stress-assisted grain growth with the above mentioned traditional driving forces has led us to consider other possible mechanisms. Low-angle boundaries are traditionally described in terms of dislocation arrays, and shear stresses are generally thought to influence low-angle boundaries by coupling to the individual dislocations in these arrays. By contrast, high-angle grain boundaries are often described in terms of coincident site lattices, and until recently the concept of coupling a shear stress to a high-angle grain boundary was relatively foreign to the materials science community. This point is illustrated in Sutton and Balluffi's book on interfaces in crystalline materials, where the authors contrast the coupling of low-angle boundaries with the sliding of high-angle boundaries. Cahn and Taylor [39] have, however, recently published a theoretical formulation describing a unified approach to grain boundary motion that illustrates how normal motion of a grain boundary can result from a shear stress applied tangential to it which results in tangential displacement of the two grains.

Winning et al. [40,41] have, in fact, experimentally measured the motion of both high- and low-angle tilt

boundaries in high-purity aluminum bicrystals under the influence of an applied stress and shown that the motion of both planar and curved high-angle boundaries can be induced by an imposed external stress. Recent MD simulations of imposed shear stresses across high-angle grain boundaries also predict the normal motion of the boundaries as a result of the applied shear stress [42]. We believe that the stress-assisted grain growth observed in the present study is yet another example of this mechanical coupling. The discontinuous nature of the grain growth is, we find, related to the fact that this mechanical coupling naturally promotes the motion of selected grain boundaries, which allows for preferential growth of the corresponding grains, while the widespread nature of the observed growth in this study suggests how effective the coupling can be in evolving the microstructure.

4.4. Role of impurities in microstructural evolution

There is strong evidence to suggest that grain boundary mobility is also influenced by impurity drag. In contrast to our samples, which retain their nanocrystalline grain size for months at room temperature, nanocrystalline Al that was chemically synthesized in a reducing atmosphere has been reported to undergo spontaneous room temperature grain growth [43]. Although the samples for our study were deposited in a vacuum chamber evacuated to a pressure of 10^{-7} torr, the incorporation of elemental amounts of oxygen cannot be ruled out given aluminum's high affinity for oxygen. In contrast to the coarsening that occurs in the chemically synthesized samples [43], the stability of the films used in the current study is itself an indication of the effect of impurities on grain boundary mobility. The observations made in this paper suggest that the as-deposited grain boundaries are pinned and then selectively unpinned under the influence of the applied stress.

This view is supported by consideration of the base pressures used to deposit the nanocrystalline films. Deposition chamber base pressures have been shown to influence the resultant microstructure during film growth; lower base pressures result in less impurities, less pinning, and larger grains [30]. Similarly, chamber base pressures have been found to affect greatly the tensile properties of the films tested in this study. Specimens deposited in a chamber with an order of magnitude higher base pressure than was used for the curves reported in Figs. 2 and 3 showed no evidence of stress-assisted grain growth or extended plasticity. Instead, these samples demonstrated mechanical behavior akin to curve 1 in Fig. 3, in which limited ductility was observed due to flow localization that occurred directly after yielding. The point is further supported by comparison with the tensile results of Haque and Saif [26,27], obtained for samples that were also deposited at a higher base pressure and did not show any evidence of grain growth or extended plasticity.

Thus it appears that an added importance of the mechanical coupling results from the fact that the pinned

boundaries cannot migrate until they are unpinned. Once unpinned by the applied stress, the motion of these boundaries would be influenced by the traditional driving forces for grain growth. With the grain size limited by thin-film effects, the process of grain growth is forced to transfer from one locale to another in a discontinuous manner: grains with favorably oriented boundaries growing first followed by those with slight less favorable orientations. It is worth noting that in situ TEM observations of rapid grain boundary migration triggered by the motion of a single dislocation into the boundary [44] further suggest that boundaries can be highly mobile once unpinned.

The observation that nominally identical specimens exhibit such different classes of behavior warrants further attention. The evidence presented here demonstrates that the difference in mechanical behavior is directly governed by the ability (or inability) of the microstructure to evolve under the influence of stress, but the exact variation between samples remains an open research question. The fact that specimens that exhibit higher strength (thus, a higher apparent driving force) do not exhibit grain growth is perhaps justified by minor changes in sample character. Although specific features such as texture, global composition, and relative number of grain differences are not observed in this study, local changes in chemistry in pure samples are known to have dramatic effects on grain boundary migration. The classic framework of impurity drag in grain boundaries developed by Cahn [45] shows that small changes in impurity composition can have a striking effect on the relation between driving force and grain boundary velocity. The inherent stability of the as-deposited films and the influence of the base pressure suggest that impurity drag is operative in this study. Direct measures of minute chemical differences and specimen-to-specimen variations in grain boundary segregation by means of high-resolution TEM electron energy loss spectroscopy and Auger microscopy have proven to be elusive [46], and it appears that quantitative atom probe mapping techniques similar to those recently proposed by Miller [47,48] will have to be developed and employed to characterize definitively grain boundary pinning. In addition, variations in grain boundary character have been shown to have an effect on the stress-coupled boundary migration mechanisms [42]. The details surrounding the characterization of these pinning and unpinning processes represent an exciting area for future research; nevertheless, the importance of stress and the effect of the grain growth on the mechanical behavior of nanocrystalline films are clear in the current study.

5. Summary and conclusions

We have conducted a set of experiments on pure nanocrystalline Al thin films to investigate the role of room temperature stress-assisted grain growth as a deformation mechanism and the effect that growth has on the overall flow response. The results of these tests indicate that the

discontinuous growth is directly coupled to the applied stress and has a dynamic effect on the macroscopic mechanical properties; ductility is enhanced at the expense of reduced strengths in comparison to tests in which no grain growth was observed. Inspection of the characteristics of the growth implies that shear stresses couple to the grain boundaries and in most cases allows the boundary to move freely away from impurity pinning atmospheres.

On the basis of the framework presented herein, we draw the following conclusions:

- The tensile behavior of nanocrystalline Al submicrometer thin films is greatly affected by grain growth. Extended ductility can be realized along with a concurrent loss in strength.
- Peak broadening measurements and TEM observations demonstrate the transition from nanocrystalline mechanisms to microcrystalline plasticity, which is facilitated by grain growth.
- This growth is a direct result of the applied stress/deformation in the film.
- Characteristics of the observed grain growth are not consistent with "traditional" driving forces (e.g. grain boundary tension, grain-to-grain strain energy differences) and appear to be related to stress-coupled boundary migration.
- The grain size and distribution play important roles in governing the plasticity in this "composite-like" structure, and modeling efforts should be focused on integrating not only the spread of the distribution but also its temporal evolution.

To date, studies of the mechanical behavior of nanocrystalline metals have concentrated on extensions of the Hall–Petch relation to smaller grain sizes or identification of the deformation mechanism or mechanisms that become operative when microcrystalline plasticity is abated. The results reported here underscore the dramatic effect that microstructural instabilities and grain growth have on the mechanical behavior of submicrometer freestanding nanocrystalline Al films. Understanding and controlling the observed grain growth may provide opportunities for improving ductility. The role of impurities and extension of this transformation to other nanocrystalline materials remains to be confirmed, but the significance of this finding with respect to the reliability of thin-film nanocrystalline devices cannot be ignored. The mechanical behavior of these structures appears to not only be different from that of microcrystalline metals but dynamic as well.

Acknowledgements

References

[1] Weertman JR. In: Koch CC, editor. Nanostructured materials: processing, properties and applications. Norwich (NY): William Andrews Publishing; 2002. p. 397.
[2] Kumar KS, Van Swygenhoven H, Suresh S. Acta Mater 2003;51:5743.
[3] Hemker KJ. Science 2003;304:221.
[4] Chen MW, Ma E, Hemker KJ. In: Gogotsi Y, editor. Nanomaterials handbook. Boca Raton (FL): Taylor & Francis/CRC Press; 2005. p. 497.
[5] Kumar KS, Suresh S, Chisholm MF, Horton JA, Wang P. Acta Mater 2003;51:387.
[6] Chen MW, Ma E, Hemker KJ, Sheng HW, Wang YM, Cheng X. Science 2003;300:1275.
[7] Hugo RC, Kung H, Weertman JR, Mitra R, Knapp JA, Follstaedt DM. Acta Mater 2003;51:1937.
[8] Shan Z, Stach EA, Wiezorek JMK, Knapp JA, Follstaedt DM, Mao SX. Science 2004;305:654.
[9] Nix WD. Metall Trans 1989;20A:2217.
[10] Fleck NA, Muller GM, Ashby MF, Hutchinson JW. Acta Mater 1994;42:475.
[11] Uchic MD, Dimiduk DM, Florando JN, Nix WD. Science 2004;305:986.
[12] Espinosa HD, Prorok BC, Peng B. J Mech Phys Solids 2004;52:667.
[13] Wang Y, Chen M, Zhou F, Ma E. Nature 2002;419:912.
[14] Lu L, Shen Y, Chen X, Qian L, Lu K. Science 2004;304:422.
[15] Van Swygenhoven H, Derlet PM, Hasnaoui A. Phys Rev B 2002;66:024101.
[16] Yamakov V, Wolf D, Phillpot SE, Mukherjee AK, Gleiter H. Nat Mater 2002;1:45.
[17] Schiøtz J, Jacobsen KW. Science 2003;301:1357.
[18] Van Swygenhoven H, Derlet PM, Froseth A. Nat Mater 2004;3:399.
[19] Legros M, Elliott BR, Rittner MN, Weertman JR, Hemker KJ. Philos Mag A 2000;80:1017.
[20] Budrovic Z, Van Swygenhoven H, Derlet PM, Van Petegem S, Schmitt B. Science 2004;304:273.
[21] Jin M, Minor AM, Stach EA, Morris Jr JW. Acta Mater 2004;52:5381.
[22] Zhang K, Weertman JR, Eastman JA. Appl Phys Lett 2004;85:5197.
[23] Chang FI, Yeh R, Lin G, Chu P, Hoffman E, Kruglick EJJ, et al. Proc SPIE 1995;2641:117.
[24] Gianola DS, Hemker KJ, Legros M, Sharpe Jr WN. TMS Lett 2004;1:149.
[25] Davis JR, editor. ASM specialty handbook: aluminum and aluminum alloys. Metals Park (OH): ASM International; 1993.
[26] Haque MA, Saif MTA. Proc Natl Acad Sci USA 2004;101:6335.
[27] Haque MA, Saif MTA. Scripta Mater 2002;47:863.
[28] Wang YM, Ma E. Acta Mater 2004;52:1699.
[29] Sanders PG, Eastman JA, Weertman JR. Acta Mater 1997;45:4019.
[30] Thompson CV. Annu Rev Mater Sci 2000;30:159.
[31] Freund LB, Suresh S. Thin film materials: stress, defect formation and surface evolution. Cambridge (UK): Cambridge University Press; 2003.
[32] Mullins WW. Acta Metall 1958;6:414.
[33] Zhou L, Zhang H, Srolovitz DJ. Acta Mater 2005;53:5273.
[34] Singh AK, Balasingh C. J Appl Phys 2001;90:2296.
[35] Morita T, Mitra R, Weertman JR. Mater Trans 2004;45:502.
[36] Zhang K, Weertman JR. Appl Phys Lett 2005;87:061921.
[37] Wang YM, Ma E. Appl Phys Lett 2004;85:2750.
[38] Gottstein G, Shvindlerman LS. Grain boundary migration in metals: thermodynamics, kinetics, applications. Boca Raton (FL): CRC Press; 1999.
[39] Cahn JW, Taylor JE. Acta Mater 2004;52:4887.
[40] Winning M, Gottstein G, Shvindlerman LS. Acta Mater 2001;49:211.

[41] Winning M, Gottstein G, Shvindlerman LS. Acta Mater 2002;50: 353.

[42] Suzuki A, Mishin Y. Mater Sci Forum 2005;502:157.

[43] Haber JA, Buhro WE. J Am Chem Soc 1998;120:10847.

[44] Soer WA, De Hosson JThM, Minor AM, Morris Jr JW, Stach EA. Acta Mater 2004;52:5783.

[45] Cahn JW. Acta Metall Mater 1962;10:789.

[46] Mendis B, Gianola DS, Hemker KJ. Unpublished results.

[47] Miller MK, Russell KF, Thompson GB. Ultramicroscopy 2005;102:287.

[48] Wu YQ, Kramer MJ, Chen Z, Ma BM, Miller MK. IEEE Trans Magn 2004;40:2886.